

Studying the $B^0 \rightarrow J/\psi h_1$ decays with $h_1(1170) - h_1(1415)$ mixing in the perturbative QCD approach

Qin Chang,^{1,2} De-Hua Yao,¹ and Xin Liu^{3,*}

¹*Institute of Particle and Nuclear Physics,
Henan Normal University, Xinxiang 453007, China*

²*Center for High Energy Physics, Henan Academy of Sciences, Zhengzhou 455004, China*

³*Department of Physics, Jiangsu Normal University, Xuzhou 221116, China*

(Dated: January 8, 2025)

Abstract

In this paper, we study the $B^0 \rightarrow J/\psi h_1$ decays for the first time by using perturbative QCD approach up to the presently known next-to-leading order accuracy. The vertex corrections present significant contribution to the amplitude. In the calculation, the mixing between two light axial-vector mesons $h_1(1170)$ and $h_1(1415)$ are also studied in detail. The observables including the branching ratios, polarization fractions and CP asymmetries are predicted and discussed explicitly. It is found that the $B^0 \rightarrow J/\psi h_1$ decays have relatively large branching fractions, which are generally at the order of $\mathcal{O}(10^{-6} \sim 10^{-3})$, and thus are possible to be observed by the LHCb and Belle-II experiments in the near future. Moreover, they are very sensitive to the mixing angle θ and can be used to test the values of θ . In addition, some ratios between the branching fractions of $B^0 \rightarrow J/\psi h_1$ decays can provide much stronger constraints on θ due to their relatively small theoretical errors. The $B^0 \rightarrow J/\psi h_1$ decays are generally dominated by the longitudinal polarization contributions, specifically, $f_L(B^0 \rightarrow J/\psi h_1) > 80\%$, except for the case that $\theta \sim 35^\circ$ and -55° . Unfortunately, the direct CP asymmetries of $B^0 \rightarrow J/\psi h_1$ decays are too small to be observed soon even if the effect of θ is considered. The future precise measurements on $B^0 \rightarrow J/\psi h_1$ decays are expected for testing these theoretical findings and exploring the interesting nature of $h_1(1170)$ and $h_1(1415)$.

* Electronic address: liuxin@jsmu.edu.cn

I. INTRODUCTION

It has been known that the decays of B meson are highly important for exploring the CP violation, which is expected to be helpful in the search of new physics beyond the Standard Model (SM) potentially. Particularly, the exclusive decays of B meson into a charmonium plus light hadrons have absorbed a lot of attention in the past decades because they play a special role in the studies of $B^0 - \bar{B}^0$ mixing phase and associated CP violation [1, 2], while our understanding on their decay mechanism is still far from satisfactory, though lots of efforts have been made to investigate these decay modes.

In the quark model, according to different spin degeneracy, the p -wave axial-vector meson contains two types of different spectroscopic notation, namely, $n^{2S+1}L_J = 1^3P_1$ and 1^1P_1 corresponding to $J^{PC} = 1^{++}$ and 1^{+-} , respectively. Intuitively, it is obvious that these two nonets have distinguishable quantum number C for the corresponding neutral mesons, i.e., $C = +$ and $C = -$ [3–5]. Experimentally, the 1^{+-} multiplets comprise $b_1(1235)(b_1)$, $h_1[h_1(1170), h_1(1415)]$ and K_{1B} , while the 1^{++} multiplets comprise $a_1(1260)(a_1)$, $f_1[f_1(1285), f_1(1420)]$ and K_{1A} [6, 7]. Some efforts have been made to study these light unflavored axial-vectors [8–12]. The considered light axial-vector h_1 states, namely, $h_1(1170)$ and $h_1(1415)$, are the important subjects of numerous experimental measurements over the past decade [13–15]. Nevertheless, the Particle Data Group (PDG) [16] continues to report “No data” on the associated decay modes for the h_1 states. Theoretically, similar to the $\eta - \eta'$ mixing in the pseudoscalar sector, the mixing scheme of the two physical h_1 mesons in the singlet-octet (SO) and quark flavor (QF) basis, respectively, can be written as [4, 17]

$$\begin{pmatrix} h_1(1170) \\ h_1(1415) \end{pmatrix} = \begin{pmatrix} \cos\theta & \sin\theta \\ -\sin\theta & \cos\theta \end{pmatrix} \begin{pmatrix} \tilde{h}_1 \\ \tilde{h}_8 \end{pmatrix} = \begin{pmatrix} \cos\alpha & \sin\alpha \\ -\sin\alpha & \cos\alpha \end{pmatrix} \begin{pmatrix} h_n \\ h_s \end{pmatrix}, \quad (1)$$

where the SO states $\tilde{h}_1 \equiv (u\bar{u} + d\bar{d} + s\bar{s})/\sqrt{3}$, $\tilde{h}_8 \equiv (u\bar{u} + d\bar{d} - 2s\bar{s})/\sqrt{6}$, and the QF states $h_n \equiv (u\bar{u} + d\bar{d})/\sqrt{2}$, $h_s \equiv s\bar{s}$, and their mixing angles θ and α obey the following relation [6, 11],

$$\theta = \alpha - \arctan\sqrt{2}. \quad (2)$$

Therefore, on the one hand, a profound understanding of the mixing angle $\theta(\alpha)$ could provide further insight into the hadronic structure of h_1 . On the other hand, with the help of Gell-Mann–Okubo (GMO) relations, the mixing angles between h_1 mesons, and between f_1 mesons have the potential to constrain the mixing angle θ_K between 3P_1 state K_{1A} and 1P_1 one K_{1B} [4, 11], and vice versa. It means that an effective constraint on the mixing angle of h_1 mesons can indirectly

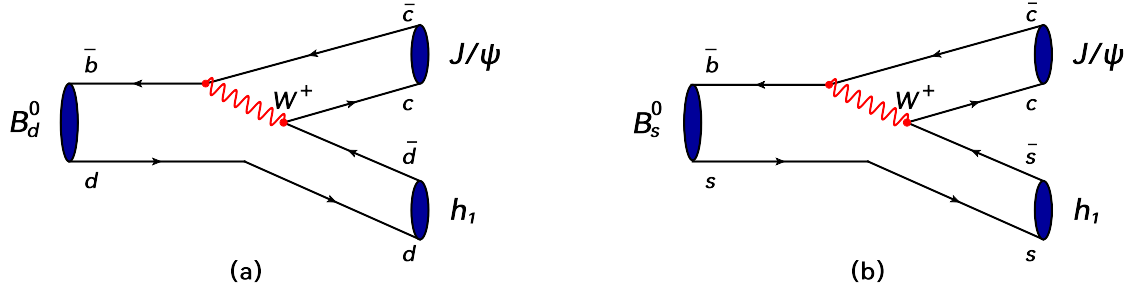


FIG. 1. (Color online) Leading quark-level Feynman diagrams for $B^0 \rightarrow J/\psi h_1$

control the range of θ_K [3, 17–23], which is helpful for analyzing the nature of $K_1(1270)$ and $K_1(1400)$. Given that the essential parameters of \tilde{h}_1 and \tilde{h}_8 have been provided in the SO mixing scheme from the hadron physics side [24], one can perform a systematic investigation of relevant B -meson weak decays involving these mentioned states.

In this article, we will systematically study the $B^0 \rightarrow J/\psi h_1$ decays (B^0 includes B_d^0 and B_s^0), and further search for new observables for determining the mixing angle θ in h_1 states. The corresponding transition processes at the quark level are illustrated in Fig. 1. Several groups have studied the B -meson decays into a charmonium state [25–42], and found that, in order to obtain reliable theoretical predictions for these color-suppressed transitions that are compatible with the current data, the next-to-leading order (NLO) QCD corrections, especially the vertex contributions, and the associated NLO Wilson coefficients, have to be taken into account in the related calculations. Besides, it is worth mentioning that the Sudakov factor for charmonia has been derived recently [43–45] and will also be taken into account in this work. Combined with the above new ingredients, we will provide theoretical predictions for the first time on several observables of $B^0 \rightarrow J/\psi h_1$, e.g., CP -averaged branching ratios, polarization fractions, relative phases, CP -violating asymmetries, and so on, by using the PQCD approach [46–51] up to NLO accuracy. Comparing with the experimental data, the branching ratios and several interesting ratios could help us to effectively constrain the range of mixing angle θ , and can provide more useful information for identifying the inner structure of the h_1 states.

This paper is organized as follows. In Sect. II, we overview briefly the mixing angle of axial-vector h_1 mesons indirectly through the Gell-Mann–Okubo mass relations, and then present the analytic expressions for the $B^0 \rightarrow J/\psi h_1$ decay amplitudes in the PQCD approach. In Sect. III, the values of requisite input parameters are collected, the theoretical results are given and the phenomenological discussions are made in detail. Finally, we give our summary in Sect. IV.

II. FORMALISM AND PERTURBATIVE QCD CALCULATIONS

A. The mixing angle

It is known that the physical eigenstates $K_1(1270)$ and $K_1(1400)$ are treated as the mixtures of K_{1A} and K_{1B} , which can be expressed as [18]

$$\begin{pmatrix} K_1(1270) \\ K_1(1400) \end{pmatrix} = \begin{pmatrix} \sin \theta_K & \cos \theta_K \\ \cos \theta_K & -\sin \theta_K \end{pmatrix} \begin{pmatrix} K_{1A} \\ K_{1B} \end{pmatrix}, \quad (3)$$

where θ_K is the mixing angle.

The value of mixing angle θ_K has been studied in the previous works. Using the early experimental information of τ decays, the authors of Ref. [18] obtain two solutions $\theta_K \approx 33^\circ$ or 57° , and present that the observed $K_1(1400)$ production dominance in the τ decay favors $\theta_K \approx 33^\circ$, while $\theta_K = (42.6 \pm 2.2)^\circ$ is obtained in Ref. [23] by using BESIII measured $M_{h_1(1415)} = (1423.2 \pm 7.6)$ MeV, which is larger than the last BESIII measurement $M_{h_1(1415)} = (1384 \pm 6)$ MeV [15]. The phenomenological analysis of the $\tau \rightarrow K_1 \nu_\tau$ decay suggested that $\theta_K \approx 45^\circ$ [19] in the relativized quark model. In Ref. [17], the author again reinforces the statement that a relatively small $\theta_K = 33^\circ$ is much more favored by the lattice and phenomenological analyses. In the nonrelativistic quark model, the range $35^\circ \leq \theta_K \leq 55^\circ$ [3] is obtained, and a refined result $\theta_K = (37.3 \pm 3.2)^\circ$ [20] is given by using the masses of $b_1(1235)$ and $a_1(1260)$ mesons. A similar result $\theta_K = (39 \pm 4)^\circ$ [21] is obtained by calculating a two-point correlation function related to θ_K within QCD sum rules. The results mentioned above are collected in Table I, and their average value is $\theta_K = 39^\circ$. Then, we would like to clarify the way to obtain the value of mixing angle θ by using θ_K .

Applying the Gell-Mann–Okubo relations (specific pedagogical conclusions can be found in Appendix A), the mass squared of the octet state can be written as

$$m_{\tilde{h}_8}^2 = \frac{4m_{K_{1B}}^2 - m_{b_1}^2}{3}, \quad (4)$$

TABLE I. Theoretical predictions for θ_K

Models	Results of θ_K
SO basis [17, 23]	$\theta_K = 33^\circ$
	$\theta_K = (42.6 \pm 2.2)^\circ$
QF basis [18, 22]	$\theta_K \approx 33^\circ$
	$\theta_K = (33.6 \pm 4.3)^\circ$
NRQM [3, 20]	$35^\circ \leq \theta_K \leq 55^\circ$
	$\theta_K = (37.3 \pm 3.2)^\circ$
QCD Sum Rules [21]	$\theta_K = (39 \pm 4)^\circ$
Relativized QM [19]	$\theta_K \approx 45^\circ$
Average	$\theta_K \approx 39^\circ$

where K_{1B} and b_1 are light meson states belonging to the 1P_1 nonet. The mixing angle θ can thus be obtained by

$$\cos^2 \theta = \frac{4m_{K_{1B}}^2 - m_{b_1}^2 - 3m_{h_1(1170)}^2}{3 \left(m_{h_1(1415)}^2 - m_{h_1(1170)}^2 \right)}, \quad \tan \theta = \frac{4m_{K_{1B}}^2 - m_{b_1}^2 - 3m_{h_1(1415)}^2}{2\sqrt{2} \left(m_{b_1}^2 - m_{K_{1B}}^2 \right)}. \quad (5)$$

The PDG results for the masses of physical states are used in our evaluation. It can be found that, for a given θ_K , the corresponding value of mixing angle θ can be extracted via the above formulae, and the value of α can also be obtained by using Eq. (2). Using some possible values of θ_K as inputs, we give the results of θ and α in Table II. The default value $\theta = 29.5^\circ$ used in our following calculations corresponds to $\theta_K = 39^\circ$. As has been shown in Eq. (1), the mixing angle θ plays an important role in the investigation of h_1 mesons, thus the effects of θ on our theoretical predictions are also discussed in our following analyses.

TABLE II. The values of mixing angles of h_1 mesons in the QF (upper) and SO (lower) basis with some possible values of θ_K as inputs.

$ \theta_K $	27°	33°	39°	45°	51°	57°
$\alpha - 90^\circ$	3.2°	-0.8°	-5.8°	-10.9°	-17.5°	-27.1°
θ	38.5°	34.5°	29.5°	24.4°	17.8°	8.2°

B. The $B^0 \rightarrow J/\psi h_1$ decays in PQCD approach

The PQCD approach is one of the popular factorization approaches on the basis of QCD, and has been widely employed to study a variety of B -meson decays. Recently, the NLO PQCD predictions of the CP -averaged branching ratios for the B^0 -meson decays into a charmonium plus light hadrons have been improved through including the important vertex corrections [28–30, 52, 53]. It makes this work a possible reference for future experimental measurements and may provide a solid theoretical basis for exploring the possible new physics beyond the SM potentially.

For the considered $B^0 \rightarrow J/\psi h_1$ decays, the effective Hamiltonian can be written as [54]

$$H_{\text{eff}} = \frac{G_F}{\sqrt{2}} \left\{ V_{cb}^* V_{cq} \left[C_1(\mu) O_1^c(\mu) + C_2(\mu) O_2^c(\mu) \right] - V_{tb}^* V_{tq} \left[\sum_{i=3}^{10} C_i(\mu) O_i(\mu) \right] \right\}, \quad (6)$$

where $q = d$ or s , the Fermi constant $G_F = 1.16639 \times 10^{-5} \text{GeV}^{-2}$, V stands for the Cabibbo-Kobayashi-Maskawa (CKM) matrix elements, and $C_i(\mu)$ are Wilson coefficients at the renormalization scale μ . The local four-quark operators $O_i (i = 1, \dots, 10)$ are given as

(1) Tree operators

$$O_1^c = (\bar{q}_\alpha c_\beta)_{V-A} (\bar{c}_\beta b_\alpha)_{V-A}, \quad O_2^c = (\bar{q}_\alpha c_\alpha)_{V-A} (\bar{c}_\beta b_\beta)_{V-A}, \quad (7)$$

(2) QCD penguin operators

$$\begin{aligned} O_3 &= (\bar{q}_\alpha b_\alpha)_{V-A} \sum_{q'} (\bar{q}'_\beta q'_\beta)_{V-A}, \quad O_4 = (\bar{q}_\alpha b_\beta)_{V-A} \sum_{q'} (\bar{q}'_\beta q'_\alpha)_{V-A}, \\ O_5 &= (\bar{q}_\alpha b_\alpha)_{V-A} \sum_{q'} (\bar{q}'_\beta q'_\beta)_{V+A}, \quad O_6 = (\bar{q}_\alpha b_\beta)_{V-A} \sum_{q'} (\bar{q}'_\beta q'_\alpha)_{V+A}, \end{aligned} \quad (8)$$

(3) Electroweak penguin operators

$$\begin{aligned} O_7 &= \frac{3}{2} (\bar{q}_\alpha b_\alpha)_{V-A} \sum_{q'} e_{q'} (\bar{q}'_\beta q'_\beta)_{V+A}, \quad O_8 = \frac{3}{2} (\bar{q}_\alpha b_\beta)_{V-A} \sum_{q'} e_{q'} (\bar{q}'_\beta q'_\alpha)_{V+A}, \\ O_9 &= \frac{3}{2} (\bar{q}_\alpha b_\alpha)_{V-A} \sum_{q'} e_{q'} (\bar{q}'_\beta q'_\beta)_{V-A}, \quad O_{10} = \frac{3}{2} (\bar{q}_\alpha b_\beta)_{V-A} \sum_{q'} e_{q'} (\bar{q}'_\beta q'_\alpha)_{V-A}, \end{aligned} \quad (9)$$

with the color indices α, β and the notations $V \pm A = \gamma_\mu (1 \pm \gamma_5)$. The index q' in the summation of the above operators runs through u, d, s, c and b . For convenience, the combination a_i of Wilson coefficients are defined as [38, 50]

$$a_1 = C_2 + \frac{C_1}{3}, \quad a_2 = C_1 + \frac{C_2}{3}, \quad (10)$$

and

$$a_i = C_i + \frac{C_{i\pm 1}}{3} \quad (i = 3 - 10), \quad (11)$$

in which the upper(lower) sign applies, when i is odd(even).

In Fig. 2, we show the typical Feynman diagrams contributing to the $B^0 \rightarrow J/\psi h_1$ decays in the PQCD approach at leading order (LO), with the first two factorizable emission diagrams and the last two non-factorizable emission ones. Consequently, analogous to the decays $B^0 \rightarrow J/\psi V$ [38], the specific forms of the factorizable emission amplitude $F_{J/\psi}^h$ (h stands for three polarizations of

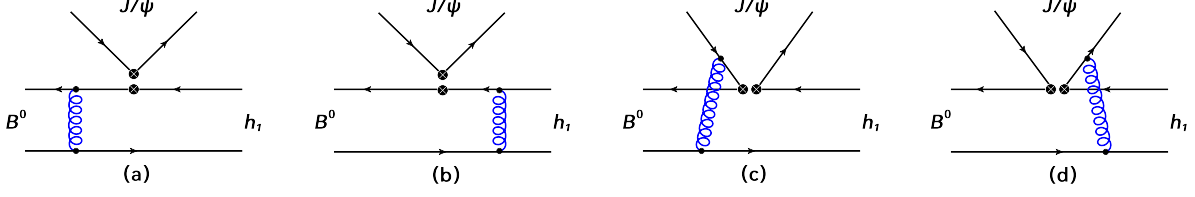


FIG. 2. (Color online) Leading order Feynman diagrams for $B^0 \rightarrow J/\psi h_1$ in the PQCD approach.

the final (axial-) vector states: longitudinal (L), normal (N), and transverse (T), respectively.) and the non-factorizable emission amplitude $M_{J/\psi}^h$ are given as

$$\begin{aligned}
F_{J/\psi}^L &= 8\pi C_F f_{J/\psi} m_{B^0}^4 \int_0^1 dx_1 dx_3 \int_0^\infty b_1 db_1 b_3 db_3 \phi_B(x_1, b_1) \left\{ \left[\sqrt{1-r_2^2} (r_A (\sqrt{1-r_2^2} \right. \right. \\
&\quad \times (2x_3 - 1) \phi_A^s(x_3) - \phi_A^t(x_3) (2x_3(r_2^2 - 1) + r_2^2 + 1)) + \phi_A(x_3) ((r_2^2 - 1)x_3 - 1) \left. \left. \right] \right. \\
&\quad \left. \times h_{fe}(x_1, x_3, b_1, b_3) E_{fe}(t_a) - \left[2r_A(1 - r_2^2) \phi_A^s(x_3) \right] h_{fe}(x_3, x_1, b_3, b_1) E_{fe}(t_b) \right\}, \quad (12)
\end{aligned}$$

$$\begin{aligned}
F_{J/\psi}^N &= 8\pi C_F f_{J/\psi} m_{B^0}^4 \int_0^1 dx_1 dx_3 \int_0^\infty b_1 db_1 b_3 db_3 \phi_B(x_1, b_1) r_2 \left\{ \left[(r_2^2 - 1) [r_A (r_2^2 - 1)x_3 \right. \right. \\
&\quad \times \phi_A^a(x_3) + \phi_A^T(x_3)] + r_A [(r_2^2 - 1)x_3 - 2] \phi_A^v(x_3) \left. \right] h_{fe}(x_1, x_3, b_1, b_3) E_{fe}(t_a) \\
&\quad \left. - r_A (r_2^2 - 1) [(r_2^2 - 1) \phi_A^a(x_3) - \phi_A^v(x_3)] h_{fe}(x_3, x_1, b_3, b_1) E_{fe}(t_b) \right\}, \quad (13)
\end{aligned}$$

$$\begin{aligned}
F_{J/\psi}^T &= 16\pi C_F f_{J/\psi} m_{B^0}^4 \int_0^1 dx_1 dx_3 \int_0^\infty b_1 db_1 b_3 db_3 \phi_B(x_1, b_1) r_2 \\
&\quad \times \left\{ \left[r_A x_3 \phi_A^v(x_3) - \phi_A^T(x_3) + r_A [(r_2^2 - 1)x_3 - 2] \phi_A^a(x_3) \right] h_{fe}(x_1, x_3, b_1, b_3) E_{fe}(t_a) \right. \\
&\quad \left. + r_A [(r_2^2 - 1) \phi_A^a(x_3) - \phi_A^v(x_3)] h_{fe}(x_3, x_1, b_3, b_1) E_{fe}(t_b) \right\}, \quad (14)
\end{aligned}$$

with $r_A = m_{\tilde{h}_{1(8)}}/m_{B^0}$ and $r_2 = m_{J/\psi}/m_{B^0}$, and

$$\begin{aligned}
M_{J/\psi}^L &= \frac{16\sqrt{6}}{3} \pi C_F m_{B^0}^4 \int_0^1 dx_1 dx_2 dx_3 \int_0^\infty b_1 db_1 b_2 db_2 \phi_B(x_1, b_1) \\
&\quad \times \left\{ \left[\sqrt{1-r_2^2} (\phi_A(x_3) - 2r_A \phi_A^t(x_3)) (r_2^2 \phi_{J/\psi}^L(x_2) (2x_2 - x_3) \right. \right. \\
&\quad \left. \left. + x_3 \phi_{J/\psi}^L(x_2) - 2r_2 r_c \phi_{J/\psi}^t(x_2)) \right] \right\} h_{nfe}(x_1, x_2, x_3, b_1, b_2) E_{nfe}(t_{nfe}), \quad (15)
\end{aligned}$$

$$\begin{aligned}
M_{J/\psi}^N &= \frac{32\sqrt{6}}{3} \pi C_F m_{B^0}^4 \int_0^1 dx_1 dx_2 dx_3 \int_0^\infty b_1 db_1 b_2 db_2 \phi_B(x_1, b_1) \\
&\quad \times \left\{ (r_2^2 - 1) \left[r_2 x_2 \phi_{J/\psi}^v(x_2) - r_c \phi_{J/\psi}^T(x_2) \right] \phi_A^T(x_3) + r_A \left[-r_c (1 + r_2^2) \phi_{J/\psi}^T(x_2) \right. \right. \\
&\quad \left. \left. + r_2 [x_2 (1 + r_2^2) + x_3 (1 - r_2^2)] \phi_{J/\psi}^v(x_2) \right] \phi_A^v(x_3) \right\} h_{nfe}(x_1, x_2, x_3, b_1, b_2) E_{nfe}(t_{nfe}), \quad (16)
\end{aligned}$$

$$\begin{aligned}
M_{J/\psi}^T &= \frac{64\sqrt{6}}{3}\pi C_F m_{B^0}^4 \int_0^1 dx_1 dx_2 dx_3 \int_0^\infty b_1 db_1 b_2 db_2 \phi_B(x_1, b_1) \\
&\times \left\{ \left[r_c \phi_{J/\psi}^T(x_2) - r_2 x_2 \phi_{J/\psi}^v(x_2) \right] \phi_A^T(x_3) + r_A \left[-r_c(1+r_2^2) \phi_{J/\psi}^T(x_2) + r_2 [x_2(1+r_2^2) \right. \right. \\
&\left. \left. + x_3(1-r_2^2)] \phi_{J/\psi}^v(x_2) \right] \phi_A^a(x_3) \right\} h_{nfe}(x_1, x_2, x_3, b_1, b_2) E_{nfe}(t_{nfe}), \quad (17)
\end{aligned}$$

where $r_c = m_c/m_{B^0}$ with m_c being the charm quark mass. For the sake of simplicity, the explicit forms of hard function $h(x_i, b_i)$, evolution function $E_i(t)$ and the running hard scale t of $F_{J/\psi}^h$ and $M_{J/\psi}^h$ in the above equations (12)-(17) can be referred to the Refs. [38, 53].

As has been emphasized in the introduction, the color-suppressed $B^0 \rightarrow J/\psi h_1$ decays should include the known NLO contributions from vertex corrections and NLO Wilson coefficients to improve the accuracy of the theoretical predictions. The corresponding vertex corrections have been shown in Fig. 3, and will be considered in our calculation. As has been pointed out in [25, 31], their effects can be absorbed into the Wilson coefficients of factorizable contributions and subsequently form a set of effective Wilson coefficients \tilde{a}_i^σ ($i = 2, 3, 5, 7, 9$) with helicities ($\sigma = 0, \pm$). The explicit expressions of \tilde{a}_i^σ can be found in Ref. [30].

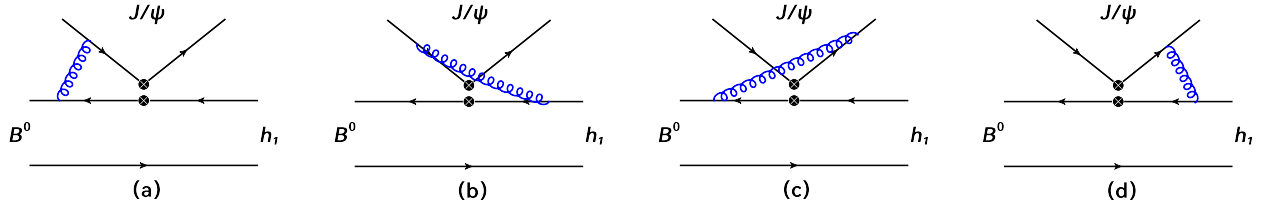


FIG. 3. (Color online) Vertex corrections to $B^0 \rightarrow J/\psi h_1$ at NLO

In the PQCD calculations at LO accuracy, we shall use the LO Wilson coefficients $C_i(m_W)$, the LO renormalization group (RG) evolution matrix $U(t, m)^{(0)}$ for the Wilson coefficient with the LO running coupling $\alpha_s(t)^{(0)}$,

$$\alpha_s(t)^{(0)} = \frac{4\pi}{\beta_0 \ln(t^2/\Lambda_{\text{QCD}}^2)}, \quad (18)$$

where $\beta_0 = (33 - 2N_f)/3$. While, the NLO Wilson coefficients $C_i(m_W)$ and the NLO RG evolution matrix $U(t, m, \alpha)$ with the running coupling $\alpha_s(t)$ at two-loop level should be used in the PQCD calculations at the NLO accuracy [54],

$$\alpha_s(t) = \frac{4\pi}{\beta_0 \ln(t^2/\Lambda_{\text{QCD}}^2)} \left\{ 1 - \frac{\beta_1}{\beta_0^2} \cdot \frac{\ln[\ln(t^2/\Lambda_{\text{QCD}}^2)]}{\ln(t^2/\Lambda_{\text{QCD}}^2)} \right\}, \quad (19)$$

where $\beta_0 = (33 - 2N_f)/3$ and $\beta_1 = (306 - 38N_f)/3$. The hadronic scale $\Lambda_{\text{QCD}}^{(4)} = 0.287$ GeV (0.326 GeV) could be obtained by using $\Lambda_{\text{QCD}}^{(5)} = 0.225$ GeV for the LO (NLO) case [54]. For the hard scale t , the lower cut-off $\mu_0 = 1.0$ GeV is chosen [55].

Using the building-blocks given above, the decay amplitudes of $B^0 \rightarrow J/\psi \tilde{h}_{1(8)}$ can then be written as

$$A^h(B_{d,s}^0 \rightarrow J/\psi \tilde{h}_{1(8)}) = F_{J/\psi}^h \left\{ V_{cb}^* V_{cd(s)} \tilde{a}_2^\sigma - V_{tb}^* V_{td(s)} \left(\tilde{a}_3^\sigma + \tilde{a}_5^\sigma + \tilde{a}_7^\sigma + \tilde{a}_9^\sigma \right) \right\} \\ + M_{J/\psi}^h \left\{ V_{cb}^* V_{cd(s)} C_2 - V_{tb}^* V_{td(s)} \left(C_4 - C_6 - C_8 + C_{10} \right) \right\}, \quad (20)$$

with the superscripts h and σ representing the polarization and helicity of the final states, respectively. Specifically, $h = L$ corresponds to a helicity $\sigma = 0$, while $h = N, T$ corresponds to helicities $\sigma = \pm$. Combining various contributions from different Feynman diagrams and the single-octet mixing scheme as given in Eq. (1), the decay amplitudes of the considered $B^0 \rightarrow J/\psi h_1$ decays with physical states could be expressed as follows,

(1) For $B_d^0 \rightarrow J/\psi h_1$ decays,

$$\mathcal{A}^h(B_d^0 \rightarrow J/\psi h_1(1170)) = A^h(B_d^0 \rightarrow J/\psi \tilde{h}_1) \frac{\cos \theta}{\sqrt{3}} + A^h(B_d^0 \rightarrow J/\psi \tilde{h}_8) \frac{\sin \theta}{\sqrt{6}}, \quad (21)$$

$$\mathcal{A}^h(B_d^0 \rightarrow J/\psi h_1(1415)) = A^h(B_d^0 \rightarrow J/\psi \tilde{h}_8) \frac{\cos \theta}{\sqrt{6}} - A^h(B_d^0 \rightarrow J/\psi \tilde{h}_1) \frac{\sin \theta}{\sqrt{3}}, \quad (22)$$

(2) For $B_s^0 \rightarrow J/\psi h_1$ decays,

$$\mathcal{A}^h(B_s^0 \rightarrow J/\psi h_1(1170)) = A^h(B_s^0 \rightarrow J/\psi \tilde{h}_1) \frac{\cos \theta}{\sqrt{3}} - 2A^h(B_s^0 \rightarrow J/\psi \tilde{h}_8) \frac{\sin \theta}{\sqrt{6}}, \quad (23)$$

$$\mathcal{A}^h(B_s^0 \rightarrow J/\psi h_1(1415)) = -2A^h(B_s^0 \rightarrow J/\psi \tilde{h}_8) \frac{\cos \theta}{\sqrt{6}} - A^h(B_s^0 \rightarrow J/\psi \tilde{h}_1) \frac{\sin \theta}{\sqrt{3}}. \quad (24)$$

III. NUMERICAL RESULTS AND DISCUSSIONS

In the numerical calculations, the meson masses, decay constants, B^0 meson lifetimes, and CKM matrix elements (Wolfenstein parameters [56]) are essential input parameters. Their values [6, 24, 57] are collected in Table III. For the nonleptonic two-body $B^0 \rightarrow J/\psi h_1$ decays, the branching fraction \mathcal{B} is defined as

$$\mathcal{B} \equiv \tau_{B^0} \cdot \Gamma(B^0 \rightarrow J/\psi h_1) = \tau_{B^0} \cdot \frac{G_F^2 |\mathbf{P}_c|}{16\pi m_{B^0}^2} \sum_{h=L,N,T} \mathcal{A}^{(h)\dagger} \mathcal{A}^{(h)}, \quad (25)$$

where τ_{B^0} is the lifetime of B^0 -meson, $|\mathbf{P}_c| \equiv |\mathbf{P}_{2z}| = |\mathbf{P}_{3z}|$ is the three-momentum of outgoing final states, and \mathcal{A}^h denotes the helicity amplitudes of $B^0 \rightarrow J/\psi h_1$ decays given in Eqs. (21)-(24).

TABLE III. The values of input parameters.

Masses (GeV)	$m_{B_d^0} = 5.28, \quad m_{B_s^0} = 5.37, \quad m_b = 4.8, \quad m_c = 1.50, \quad m_{J/\psi} = 3.097,$ $m_{h_1(1170)} = 1.166, \quad m_{h_1(1415)} = 1.409, \quad m_{\tilde{h}_1} = 1.23, \quad m_{\tilde{h}_8} = 1.36$
Decay constants (GeV)	$f_{B_d^0} = 0.21 \pm 0.02, \quad f_{B_s^0} = 0.23 \pm 0.02, \quad f_{J/\psi} = 0.405 \pm 0.014,$ $f_{\tilde{h}_1} = 0.180 \pm 0.012, \quad f_{\tilde{h}_8} = 0.190 \pm 0.010$
B -meson lifetimes (ps)	$\tau_{B_d^0} = 1.519 \pm 0.004, \quad \tau_{B_s^0} = 1.520 \pm 0.005$
CKM parameters	$A = 0.826_{-0.015}^{+0.018}, \quad \lambda = 0.22500 \pm 0.00067, \quad \bar{\rho} = 0.159 \pm 0.010,$ $\bar{\eta} = 0.348 \pm 0.010$

Using the decay amplitudes and input parameters given above, our LO and NLO PQCD predictions for the CP -averaged branching fractions of $B^0 \rightarrow J/\psi h_1$ decays, accompanied with multiple uncertainties, are given in Table IV. The first four theoretical errors are induced by the shape parameter $\omega_{B_d^0} = 0.40 \pm 0.04$ GeV or $\omega_{B_s^0} = 0.50 \pm 0.05$ GeV in the B^0 -meson distribution amplitude, the decay constant f_M of two outgoing final states as presented in Table III, the charm quark mass $m_c = 1.50 \pm 0.15$ GeV, and the Gegenbauer moments a_1^\parallel and a_2^\perp (see Eq. (B7)) in the light-cone distribution amplitudes of the h_1 mesons, respectively. The last error arises from factor $a_t = 1.0 \pm 0.2$ describing the possible higher-order corrections, which are characterized through simply varying the running hard scale t_{\max} with 20% in the hard kernel. From Table IV, it can be clearly seen that the dominated uncertainties arise mainly from the hadronic parameters such as the Gegenbauer moments and the decay constants.

 TABLE IV. The LO and NLO PQCD predictions of the CP -averaged branching ratios for the $B^0 \rightarrow J/\psi h_1$ decays.

Decay modes	LO	NLO
$B_d^0 \rightarrow J/\psi h_1(1170)$	$(6.55_{-1.35-0.91-0.90-1.31-1.60}^{+1.78+0.96+1.20+1.58+2.23}) \times 10^{-5}$	$(9.54_{-1.87-1.54-0.74-2.43-0.38}^{+2.39+1.65+0.72+2.83+0.26}) \times 10^{-5}$
$B_d^0 \rightarrow J/\psi h_1(1415)$	$(1.12_{-0.26-0.08-0.08-0.17-0.32}^{+0.36+0.08+0.14+0.22+0.44}) \times 10^{-6}$	$(1.32_{-0.26-0.15-0.13-0.35-0.07}^{+0.35+0.17+0.14+0.41+0.04}) \times 10^{-6}$
$B_s^0 \rightarrow J/\psi h_1(1170)$	$(0.90_{-0.20-0.23-0.03-0.22-0.05}^{+0.27+0.26+0.09+0.26+0.08}) \times 10^{-5}$	$(1.50_{-0.32-0.39-0.03-0.38-0.02}^{+0.42+0.44+0.01+0.44+0.01}) \times 10^{-5}$
$B_s^0 \rightarrow J/\psi h_1(1415)$	$(1.05_{-0.23-0.14-0.06-0.30-0.04}^{+0.29+0.14+0.09+0.36+0.07}) \times 10^{-3}$	$(1.74_{-0.39-0.22-0.02-0.51-0.02}^{+0.50+0.26+0.01+0.61+0.01}) \times 10^{-3}$

Comparing the numerical results at LO with the ones at NLO, we find that the NLO contributions from vertex corrections can significantly enhance the branching ratios due to the corrected effective Wilson coefficient \tilde{a}_2 being much larger than the original one a_2 [25, 31]. Furthermore, we also note that the error arisen from the running hard scale t can be reduced from 30% to 5%. Therefore, the subsequent numerical results and phenomenological analyses are all at the presently known NLO level, unless otherwise specified.

Adding the above-mentioned errors in quadrature, the NLO PQCD results for $\mathcal{B}(B^0 \rightarrow J/\psi h_1)$ can be written as

(i) For $\bar{b} \rightarrow c\bar{c}\bar{d}$ decays,

$$\mathcal{B}(B_d^0 \rightarrow J/\psi h_1(1170)) = 9.54_{-3.53}^{+4.13} \times 10^{-5}, \quad \mathcal{B}(B_d^0 \rightarrow J/\psi h_1(1415)) = 1.32_{-0.48}^{+0.58} \times 10^{-6}, \quad (26)$$

(ii) For $\bar{b} \rightarrow c\bar{c}\bar{s}$ decays,

$$\mathcal{B}(B_s^0 \rightarrow J/\psi h_1(1170)) = 1.50_{-0.63}^{+0.75} \times 10^{-5}, \quad \mathcal{B}(B_s^0 \rightarrow J/\psi h_1(1415)) = 1.74_{-0.68}^{+0.83} \times 10^{-3}. \quad (27)$$

From these results, it can be found that $B^0 \rightarrow J/\psi h_1$ decays have relatively large branching ratios, which are around $10^{-6} \sim 10^{-3}$, and are possible to be measured at the ongoing LHCb and Belle-II experiments in the near future.

TABLE V. Decay amplitudes (in units of 10^{-3} GeV^3) of the $B^0 \rightarrow J/\psi h_1$ modes with three polarizations in the PQCD approach.

Decays		$\mathcal{A}_{B_d^0}$		$\mathcal{A}_{B_s^0}$	
		Tree	Penguin	Tree	Penguin
$J/\psi h_1(1170)$	\mathcal{A}_L	$-0.125 - i0.529$	$-0.002 - i0.013$	$0.026 + i0.212$	$-0.001 + i0.006$
	\mathcal{A}_N	$-0.032 - i0.143$	$0.000 - i0.004$	$0.026 + i0.034$	$0.000 + i0.001$
	\mathcal{A}_T	$-0.110 - i0.394$	$-0.001 - i0.010$	$0.080 + i0.104$	$0.001 + i0.003$
$J/\psi h_1(1415)$	\mathcal{A}_L	$-0.021 - i0.064$	$-0.000 - i0.002$	$-0.296 - i2.422$	$0.003 - i0.061$
	\mathcal{A}_N	$-0.002 - i0.020$	$0.000 - i0.001$	$-0.235 - i0.410$	$-0.005 - i0.010$
	\mathcal{A}_T	$-0.008 - i0.053$	$0.000 - i0.002$	$-0.705 - i1.227$	$-0.014 - i0.030$

In order to see clearly the interferences between two final states $J/\psi\tilde{h}_1$ and $J/\psi\tilde{h}_8$, we also give the numerical results of polarization amplitudes of $B^0 \rightarrow J/\psi h_1$ and $B^0 \rightarrow J/\psi\tilde{h}_{1,8}$ modes in Tables V and VI, respectively. Meanwhile, the amplitudes induced by the tree operators and the

TABLE VI. Same as Table V but for neutral B -meson decays into $J/\psi\tilde{h}_1$ and $J/\psi\tilde{h}_8$.

Decays		$A_{B_d^0}$		$A_{B_s^0}$	
Contributions		Tree	Penguin	Tree	Penguin
$J/\psi\tilde{h}_1$	\mathcal{A}_L	$-0.170 - i0.743$	$-0.003 - i0.018$	$0.292 + i2.384$	$-0.003 + i0.060$
	\mathcal{A}_N	$-0.047 - i0.198$	$0.000 - i0.005$	$0.239 + i0.401$	$0.005 + i0.010$
	\mathcal{A}_T	$-0.159 - i0.549$	$-0.001 - i0.014$	$0.721 + i1.204$	$0.014 + i0.029$
$J/\psi\tilde{h}_8$	\mathcal{A}_L	$-0.195 - i0.775$	$-0.003 - i0.019$	$0.300 + i2.454$	$-0.003 + i0.061$
	\mathcal{A}_N	$-0.043 - i0.214$	$0.000 - i0.006$	$0.234 + i0.401$	$0.005 + i0.010$
	\mathcal{A}_T	$-0.151 - i0.549$	$-0.001 - i0.015$	$0.704 + i1.245$	$0.014 + i0.030$

penguin operators are also listed. These numerical results indicate that the considered decay modes are dominated by the tree diagrams, with only a few percent of penguin contaminations. Combined with Eqs. (21)-(24), it is evident to observe that the constructive or destructive interferences with different extents in the considered decays could vary with the mixing angle θ in the SO basis. Thus, in order to show the effects of mixing angle θ , we plot the dependence of NLO PQCD predictions of $\mathcal{B}(B^0 \rightarrow J/\psi h_1)$ on the mixing angle $\theta \in [-\frac{\pi}{2}, \frac{\pi}{2}]$ in Fig. 4. It can be clearly seen that the $\mathcal{B}(B^0 \rightarrow J/\psi h_1)$ are very sensitive to the mixing angle θ . From the Eqs. (21)-(24) and Fig. 4, it can be clearly seen that the interference between the $B_s^0 \rightarrow J/\psi\tilde{h}_1$ and $B_s^0 \rightarrow J/\psi\tilde{h}_8$ decay amplitudes consequently leads to that $\mathcal{B}(B_s^0 \rightarrow J/\psi h_1(1170), B_d^0 \rightarrow J/\psi h_1(1415))$ are significantly reduced, while $\mathcal{B}(B_d^0 \rightarrow J/\psi h_1(1170), B_s^0 \rightarrow J/\psi h_1(1415))$ are enhanced, at $\theta \sim 29.5^\circ$. Therefore, the experimental measurement of these branching fractions would play an important role in testing the value of θ .

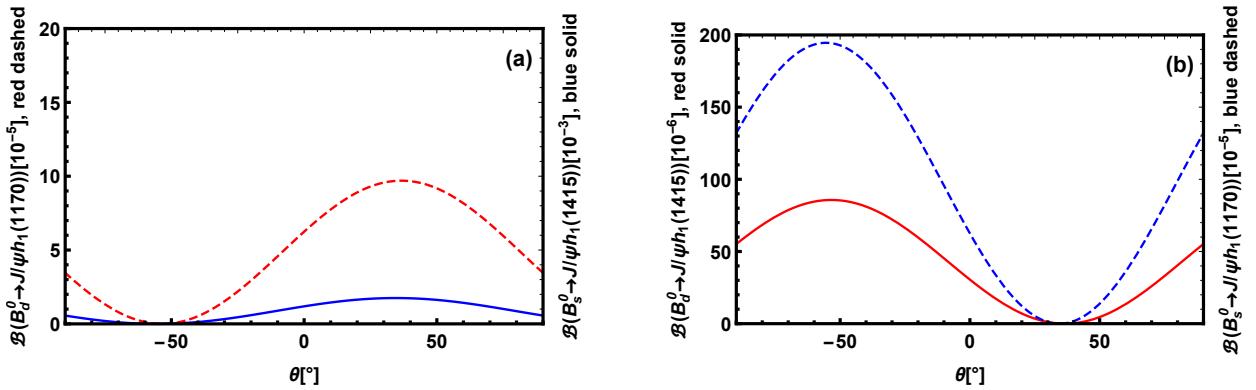


FIG. 4. (Color online) The dependence of $\mathcal{B}(B^0 \rightarrow J/\psi h_1)$ on the mixing angle θ in the PQCD approach.

There are several unflavored light mesons, such as $a_1(1260)$, $f_1(1285)$, $\eta(1405)$, $f_1(1420)$ and $\eta(1475)$, that are known to decay into $K_S^0 K^\pm \pi^\mp$, and that could in principle be produced in B^0 meson decays alongside charmonium states [58]. For the $h_1(1415)$ state below $1500 \text{ MeV}/c^2$, the process $h_1(1415) \rightarrow K_S^0 K^\pm \pi^\mp$ has not been measured [6]. As discussed in Ref. [11], the decay rate of the dominant decay mode is $\mathcal{B}(h_1(1415) \rightarrow K^* \bar{K}) = 0.415 \pm 0.085$, then the branching fraction $\mathcal{B}(h_1(1415) \rightarrow K_S^0 K^\pm \pi^\mp) \approx 0.277 \pm 0.056$ can be naively determined due to the isospin conservation for the strong decays $K^* \rightarrow K\pi$. Based on the narrow-width-approximation (NWA), we can obtain the branching fractions of $B^0 \rightarrow J/\psi h_1(1415) (\rightarrow K_S^0 K^\pm \pi^\mp)$ decays,

$$\begin{aligned} \mathcal{B}(B_s^0 \rightarrow J/\psi(K_S^0 K^+ \pi^-)_{h_1(1415)}) &\equiv \mathcal{B}(B_s^0 \rightarrow J/\psi h_1(1415)) \\ &\cdot \mathcal{B}(h_1(1415) \rightarrow K_S^0 K^+ \pi^-) \approx 0.48_{-0.21}^{+0.25} \times 10^{-3}, \end{aligned} \quad (28)$$

$$\begin{aligned} \mathcal{B}(B_d^0 \rightarrow J/\psi(K_S^0 K^+ \pi^-)_{h_1(1415)}) &\equiv \mathcal{B}(B_d^0 \rightarrow J/\psi h_1(1415)) \\ &\cdot \mathcal{B}(h_1(1415) \rightarrow K_S^0 K^+ \pi^-) \approx 0.37_{-0.15}^{+0.18} \times 10^{-6}, \end{aligned} \quad (29)$$

where the error arising from the $h_1(1415)$ decay width has been taken into account. As have been given in Ref. [30], the theoretical results for above processes through $f_1(1420)$ resonance showed that,

$$\mathcal{B}(B_s^0 \rightarrow J/\psi(K_S^0 K^+ \pi^-)_{f_1(1420)}) \approx 0.73_{-0.28}^{+0.36} \times 10^{-3}, \quad (30)$$

$$\mathcal{B}(B_d^0 \rightarrow J/\psi(K_S^0 K^+ \pi^-)_{f_1(1420)}) \approx 1.27_{-0.68}^{+0.88} \times 10^{-6}. \quad (31)$$

While, the $B^0 \rightarrow J/\psi K_S^0 K^\pm \pi^\mp$ decays have been measured by the LHCb Collaboration, their branching ratios are [58]

$$\mathcal{B}(B_s^0 \rightarrow J/\psi K_S^0 K^+ \pi^-)_{\text{Exp}} = (0.91 \pm 0.09) \times 10^{-3}, \quad (32)$$

$$\mathcal{B}(B_d^0 \rightarrow J/\psi K_S^0 K^+ \pi^-)_{\text{Exp}} < 2.01 \times 10^{-5}. \quad (33)$$

For the well measured $B_s^0 \rightarrow J/\psi K_S^0 K^+ \pi^-$ decay, comparing the theoretical results given in Eqs. (28) and (30) with data given in Eq. (32), it can be found that the sum of the branching fractions of $B_s^0 \rightarrow J/\psi K_S^0 K^+ \pi^-$ decay via $h_1(1415)$ and $f_1(1420)$ resonances is approximately consistent with the LHCb measurement of $\mathcal{B}(B_s^0 \rightarrow J/\psi K_S^0 K^+ \pi^-)$. However, considering the presently unknown interferences between the amplitudes from two different $f_1(1420)$ and $h_1(1415)$ resonant states, an accurate quantification of the $h_1(1415)$ resonance contributing to the $m(K_S^0 K^\pm \pi^\mp)$ distribution still requires further experimental and/or theoretical examinations on the interference effects.

As has been shown in Table IV, the branching fractions of the $B^0 \rightarrow J/\psi h_1$ decays have relatively large theoretical uncertainties due to the various hadronic input parameters. Generally, the theoretical errors caused by the same hadronic input parameters can be significantly cancelled by introducing some ratios. For instance, one can define the following two ratios,

$$R_d^{\text{SO}} \equiv \frac{\mathcal{B}(B_d^0 \rightarrow J/\psi h_1(1170))}{\mathcal{B}(B_d^0 \rightarrow J/\psi h_1(1415))} = \frac{\Phi(m_{B_d^0}, m_{J/\psi}, m_{h_1(1170)})}{\Phi(m_{B_d^0}, m_{J/\psi}, m_{h_1(1415)})} \cdot \frac{\left| \frac{\cos\theta}{\sqrt{3}} \cdot A(B_d^0 \rightarrow J/\psi \tilde{h}_1) + \frac{\sin\theta}{\sqrt{6}} \cdot A(B_d^0 \rightarrow J/\psi \tilde{h}_8) \right|^2}{\left| -\frac{\sin\theta}{\sqrt{3}} \cdot A(B_d^0 \rightarrow J/\psi \tilde{h}_1) + \frac{\cos\theta}{\sqrt{6}} \cdot A(B_d^0 \rightarrow J/\psi \tilde{h}_8) \right|^2}, \quad (34)$$

$$R_s^{\text{SO}} \equiv \frac{\mathcal{B}(B_s^0 \rightarrow J/\psi h_1(1415))}{\mathcal{B}(B_s^0 \rightarrow J/\psi h_1(1170))} = \frac{\Phi(m_{B_s^0}, m_{J/\psi}, m_{h_1(1415)})}{\Phi(m_{B_s^0}, m_{J/\psi}, m_{h_1(1170)})} \cdot \frac{\left| -\frac{\sin\theta}{\sqrt{3}} \cdot A(B_s^0 \rightarrow J/\psi \tilde{h}_1) - 2 \cdot \frac{\cos\theta}{\sqrt{6}} \cdot A(B_s^0 \rightarrow J/\psi \tilde{h}_8) \right|^2}{\left| \frac{\cos\theta}{\sqrt{3}} \cdot A(B_s^0 \rightarrow J/\psi \tilde{h}_1) - 2 \cdot \frac{\sin\theta}{\sqrt{6}} \cdot A(B_s^0 \rightarrow J/\psi \tilde{h}_8) \right|^2}, \quad (35)$$

where the phase space factor is given as $\Phi(a, b, c) = [(a^2 - (b+c)^2)(a^2 - (b-c)^2)]^{\frac{1}{2}}$ [59]. It can be found that, these ratios can be used to test or extract the values of mixing angle θ approximately in a model independent way if $A(B^0 \rightarrow J/\psi \tilde{h}_1) = A(B^0 \rightarrow J/\psi \tilde{h}_8)$, which is approximately valid as has been shown through the numerical results given in Table VI. Our numerical results are

$$R_d^{\text{SO}} = 72.27_{-4.53}^{+3.59}, \quad R_s^{\text{SO}} = 116.52_{-10.96}^{+10.46}. \quad (36)$$

It can be obviously found that the theoretical errors are significantly reduced. Moreover, in order to obtain a more intuitive interpretation, one can employ a more convenient and intuitive form by extending the ratios to the QF basis, which can be exactly derived as

$$R_d^{\text{QF}} \equiv \frac{\mathcal{B}(B_d^0 \rightarrow J/\psi h_1(1170))}{\mathcal{B}(B_d^0 \rightarrow J/\psi h_1(1415))} = \frac{\Phi(m_{B_d}, m_{J/\psi}, m_{h_1(1170)})}{\Phi(m_{B_d}, m_{J/\psi}, m_{h_1(1415)})} \cdot \cot^2 \alpha, \quad (37)$$

$$R_s^{\text{QF}} \equiv \frac{\mathcal{B}(B_s^0 \rightarrow J/\psi h_1(1415))}{\mathcal{B}(B_s^0 \rightarrow J/\psi h_1(1170))} = \frac{\Phi(m_{B_s}, m_{J/\psi}, m_{h_1(1415)})}{\Phi(m_{B_s}, m_{J/\psi}, m_{h_1(1170)})} \cdot \cot^2 \alpha, \quad (38)$$

where the ratios R_d^{QF} and R_s^{QF} are independent on the decay amplitudes. They could provide a much more convenient and clear way to extract the angle α when they are measured by the future experiments. The mixing angle θ can be further obtained via Eq. (2). Beside of the ratios mentioned above, the ratios defined as

$$R_{ds}^{\text{SO}}[h_1(1170)] \equiv \frac{\mathcal{B}(B_d^0 \rightarrow J/\psi h_1(1170))}{\mathcal{B}(B_s^0 \rightarrow J/\psi h_1(1170))}, \quad R_{sd}^{\text{SO}}[h_1(1415)] \equiv \frac{\mathcal{B}(B_s^0 \rightarrow J/\psi h_1(1415))}{\mathcal{B}(B_d^0 \rightarrow J/\psi h_1(1415))}, \quad (39)$$

can also be used to constrain the absolute value of mixing angle θ . Our numerical results are

$$R_{ds}^{\text{SO}}[h_1(1170)] \approx 6.38_{-0.89}^{+1.17}, \quad R_{sd}^{\text{SO}}[h_1(1415)] \approx 13.18_{-1.92}^{+2.02} \times 10^2, \quad (40)$$

in which, all errors arising from various input parameters have been added in quadrature.

Now, we turn to investigate the polarization fractions of the $B^0 \rightarrow J/\psi h_1$ decays. Based on the helicity amplitudes given in Eqs. (21)-(24), we can equivalently define a set of transversity amplitudes as follows,

$$\mathcal{A}_L = m_{B^0}^2 \mathcal{A}_L, \quad \mathcal{A}_{\parallel} = \sqrt{2} m_{B^0}^2 \mathcal{A}_N, \quad \mathcal{A}_{\perp} = m_{J/\psi} m_{h_1} \sqrt{2(\kappa^2 - 1)} \mathcal{A}_T, \quad (41)$$

for the longitudinal, parallel and perpendicular polarization states, respectively, with the ratio $\kappa = P_2 \cdot P_3 / (m_{J/\psi} m_{h_1})$. Then, we can define the polarization fractions as

$$f_{L,\parallel,\perp} \equiv \frac{|\mathcal{A}_{L,\parallel,\perp}|^2}{|\mathcal{A}_L|^2 + |\mathcal{A}_{\parallel}|^2 + |\mathcal{A}_{\perp}|^2}, \quad f_T \equiv \frac{|\mathcal{A}_{\parallel}|^2 + |\mathcal{A}_{\perp}|^2}{|\mathcal{A}_L|^2 + |\mathcal{A}_{\parallel}|^2 + |\mathcal{A}_{\perp}|^2} = f_{\parallel} + f_{\perp}, \quad (42)$$

which obviously satisfy the relation $f_L + f_{\parallel} + f_{\perp} = f_L + f_T = 1$. In addition, the relative phases ϕ_{\parallel} and ϕ_{\perp} (in units of rad) are defined as

$$\phi_{\parallel} = \arg \frac{\mathcal{A}_{\parallel}}{\mathcal{A}_L}, \quad \phi_{\perp} = \arg \frac{\mathcal{A}_{\perp}}{\mathcal{A}_L}. \quad (43)$$

TABLE VII. Theoretical predictions for the polarization observables of the $B_d^0 \rightarrow J/\psi h_1$ decays.

Observables	$B_d^0 \rightarrow J/\psi h_1(1170)$	$B_d^0 \rightarrow J/\psi h_1(1415)$
$f_L(\%)$	$81.3_{-0.3-0.1-1.8-4.5-0.2}^{+0.3+0.1+1.3+3.6+0.2}$	$80.3_{-0.6-0.1-1.7-3.8-0.4}^{+0.6+0.1+0.9+3.1+0.3}$
$f_{\parallel}(\%)$	$11.8_{-0.2-0.1-0.6-2.1-0.1}^{+0.2+0.1+0.9+2.7+0.1}$	$13.5_{-0.5-0.1-0.3-2.0-0.1}^{+0.5+0.1+1.1+2.4+0.2}$
$f_{\perp}(\%)$	$6.9_{-0.1-0.0-0.7-1.5-0.1}^{+0.1+0.0+0.9+1.9+0.1}$	$6.2_{-0.2-0.0-0.6-1.1-0.1}^{+0.2+0.0+0.7+1.5+0.2}$
$\phi_{\parallel}(\text{rad})$	$3.16_{-0.02-0.00-0.13-0.10-0.00}^{+0.02+0.00+0.11+0.12+0.01}$	$3.36_{-0.03-0.01-0.10-0.11-0.01}^{+0.02+0.01+0.07+0.13+0.01}$
$\phi_{\perp}(\text{rad})$	$3.10_{-0.01-0.00-0.12-0.10-0.00}^{+0.01+0.00+0.09+0.13+0.00}$	$3.30_{-0.01-0.01-0.09-0.11-0.01}^{+0.01+0.01+0.06+0.14+0.01}$
$A_{\text{CP}}^{\text{dir},L}(10^{-2})$	$-0.81_{-0.05-0.02-0.02-0.09-0.44}^{+0.04+0.02+0.02+0.06+0.40}$	$-1.05_{-0.06-0.03-0.05-0.10-0.44}^{+0.06+0.03+0.07+0.08+0.43}$
$A_{\text{CP}}^{\text{dir},\parallel}(10^{-2})$	$-1.17_{-0.07-0.03-0.07-0.10-0.45}^{+0.07+0.03+0.07+0.12+0.42}$	$-1.27_{-0.09-0.04-0.09-0.12-0.49}^{+0.08+0.04+0.10+0.14+0.45}$
$A_{\text{CP}}^{\text{dir},\perp}(10^{-2})$	$-0.99_{-0.07-0.02-0.09-0.09-0.42}^{+0.06+0.02+0.07+0.11+0.39}$	$-1.18_{-0.09-0.03-0.14-0.10-0.44}^{+0.09+0.03+0.13+0.15+0.43}$

TABLE VIII. Same as Table VII but for $B_s^0 \rightarrow J/\psi h_1$ decays.

Decay modes	$B_s^0 \rightarrow J/\psi h_1(1170)$	$B_s^0 \rightarrow J/\psi h_1(1415)$
$f_L(\%)$	$87.6^{+0.3+0.1+2.7+4.5+0.2}_{-0.2-0.1-2.7-5.7-0.2}$	$89.4^{+0.3+0.0+2.6+4.3+0.1}_{-0.3-0.0-2.8-5.9-0.1}$
$f_{\parallel}(\%)$	$7.1^{+0.2+0.1+1.6+3.3+0.1}_{-0.2-0.1-1.5-2.6-0.1}$	$6.7^{+0.2+0.0+1.8+3.7+0.1}_{-0.2-0.0-1.6-2.7-0.1}$
$f_{\perp}(\%)$	$5.3^{+0.1+0.1+1.1+2.4+0.1}_{-0.1-0.0-1.2-1.9-0.1}$	$3.9^{+0.1+0.0+1.0+2.2+0.1}_{-0.1-0.0-1.0-1.6-0.1}$
$\phi_{\parallel}(\text{rad})$	$2.61^{+0.01+0.01+0.14+0.11+0.01}_{-0.01-0.01-0.19-0.07-0.01}$	$2.74^{+0.01+0.00+0.16+0.16+0.01}_{-0.01-0.00-0.19-0.11-0.00}$
$\phi_{\perp}(\text{rad})$	$2.61^{+0.01+0.01+0.15+0.11+0.01}_{-0.01-0.01-0.18-0.08-0.01}$	$2.74^{+0.01+0.00+0.16+0.17+0.01}_{-0.01-0.00-0.19-0.11-0.00}$
$A_{\text{CP}}^{\text{dir,L}}(10^{-4})$	$1.65^{+0.02+0.03+0.48+0.01+1.86}_{-0.10-0.02-0.27-0.01-1.46}$	$1.37^{+0.00+0.01+0.10+0.00+1.97}_{-0.01-0.01-0.09-0.00-1.66}$
$A_{\text{CP}}^{\text{dir,}\parallel}(10^{-4})$	$1.64^{+0.15+0.08+0.34+0.27+1.12}_{-0.14-0.06-0.20-0.71-1.18}$	$0.52^{+0.09+0.00+0.11+0.63+1.39}_{-0.07-0.00-0.00-0.96-1.20}$
$A_{\text{CP}}^{\text{dir,}\perp}(10^{-4})$	$1.55^{+0.09+0.08+0.21+0.29+1.11}_{-0.09-0.06-0.11-0.72-0.97}$	$0.58^{+0.09+0.01+0.07+0.59+1.37}_{-0.09-0.01-0.05-0.97-1.21}$

Our numerical results for the polarization observables of $B^0 \rightarrow J/\psi h_1$ decays are given in Tables VII and VIII. Adding the errors in quadrature, the results of polarization fractions can be simplified as

$$f_L(B_d^0 \rightarrow J/\psi h_1(1170)) = (81.3^{+3.9}_{-4.9})\%, \quad f_T(B_d^0 \rightarrow J/\psi h_1(1170)) = (18.7^{+3.5}_{-2.7})\%, \quad (44)$$

$$f_L(B_d^0 \rightarrow J/\psi h_1(1415)) = (80.3^{+3.2}_{-4.3})\%, \quad f_T(B_d^0 \rightarrow J/\psi h_1(1415)) = (19.7^{+3.1}_{-2.4})\%, \quad (45)$$

and

$$f_L(B_s^0 \rightarrow J/\psi h_1(1170)) = (87.6^{+5.3}_{-6.3})\%, \quad f_T(B_s^0 \rightarrow J/\psi h_1(1170)) = (12.4^{+4.5}_{-3.7})\%, \quad (46)$$

$$f_L(B_s^0 \rightarrow J/\psi h_1(1415)) = (89.4^{+5.0}_{-6.5})\%, \quad f_T(B_s^0 \rightarrow J/\psi h_1(1415)) = (10.6^{+4.7}_{-3.6})\%, \quad (47)$$

It can be found that $f_L(B^0 \rightarrow J/\psi h_1)$ are generally larger than 80%, which indicate that $B^0 \rightarrow J/\psi h_1$ decays are dominated by the longitudinal contributions. The dependence of $f_L(B^0 \rightarrow J/\psi h_1)$ on the mixing angle θ is shown in Fig. 5. It can be found that the polarization fractions generally are not sensitive to the value of θ , except at $\theta \sim 35^\circ$ for $B_d^0 \rightarrow J/\psi h_1(1415)$ and $B_s^0 \rightarrow J/\psi h_1(1170)$ decays and at $\theta \sim -55^\circ$ for $B_d^0 \rightarrow J/\psi h_1(1170)$ and $B_s^0 \rightarrow J/\psi h_1(1415)$ decays. Thus, the polarization would present a very strong constraint on θ if a relatively small $f_L(B^0 \rightarrow J/\psi h_1)$ is observed by the experiments.

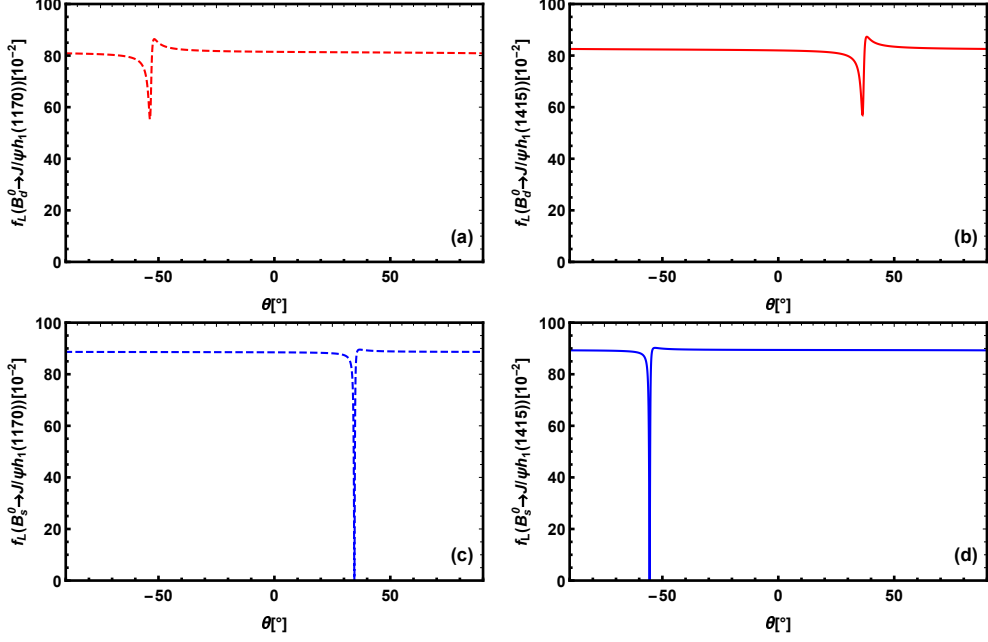


FIG. 5. (Color online) The dependence of $f_L(B^0 \rightarrow J/\psi h_1)$ on the mixing angle θ in the PQCD approach.

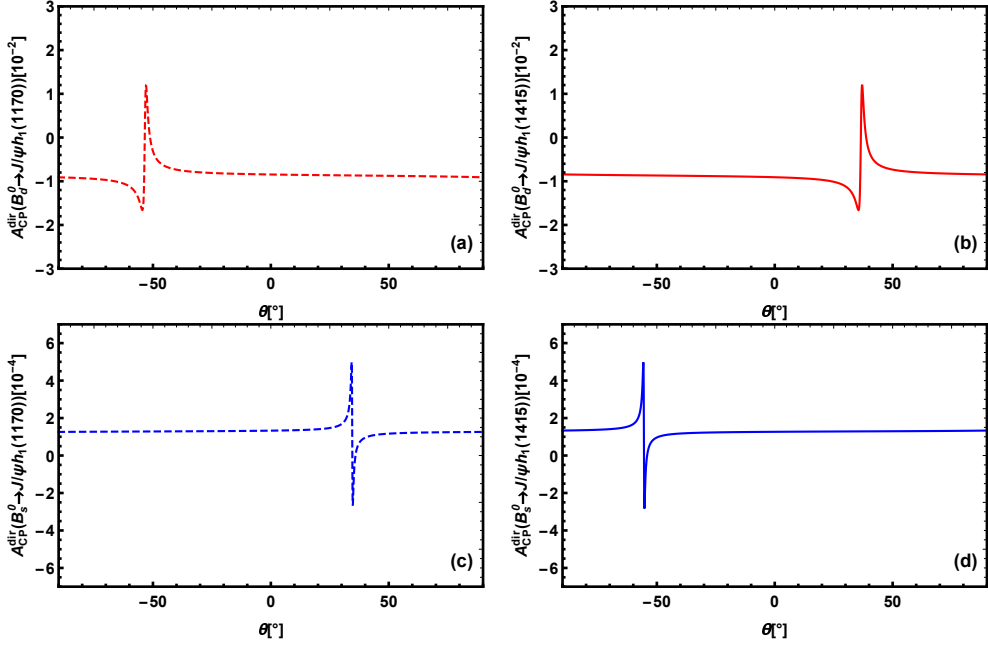


FIG. 6. (Color online) The dependence of $A_{\text{CP}}^{\text{dir}}(B^0 \rightarrow J/\psi h_1)$ on the mixing angle θ in the PQCD approach.

The direct CP asymmetry $A_{\text{CP}}^{\text{dir}}$ of $B^0 \rightarrow J/\psi h_1$ decays is defined as

$$A_{\text{CP}}^{\text{dir}} \equiv \frac{|\overline{\mathcal{A}}(\overline{B}^0 \rightarrow \overline{f})|^2 - |\mathcal{A}(B^0 \rightarrow f)|^2}{|\overline{\mathcal{A}}(\overline{B}^0 \rightarrow \overline{f})|^2 + |\mathcal{A}(B^0 \rightarrow f)|^2}, \quad (48)$$

where \mathcal{A} represents the decay amplitudes of $B^0 \rightarrow J/\psi h_1$, while $\overline{\mathcal{A}}$ describe the corresponding charge conjugation ones. Meanwhile, according to Ref. [60], the direct CP asymmetries in each polarization can also be studied as

$$A_{\text{CP}}^{\text{dir},\alpha} = \frac{\overline{f}_\alpha - f_\alpha}{\overline{f}_\alpha + f_\alpha} \quad (\alpha = L, \parallel, \perp), \quad (49)$$

where \overline{f}_α is the polarization fraction for the corresponding \overline{B}^0 decays in Eq.(42). Using Eq.(48), our numerical predictions for the direct CP asymmetries of the $B^0 \rightarrow J/\psi h_1$ decays in the PQCD approach are

$$A_{\text{CP}}^{\text{dir}}(B_d^0 \rightarrow J/\psi h_1(1170)) = -0.86_{-0.44}^{+0.41} \times 10^{-2}, \quad A_{\text{CP}}^{\text{dir}}(B_d^0 \rightarrow J/\psi h_1(1415)) = -1.09_{-0.46}^{+0.45} \times 10^{-2}, \quad (50)$$

$$A_{\text{CP}}^{\text{dir}}(B_s^0 \rightarrow J/\psi h_1(1170)) = 1.64_{-1.44}^{+1.81} \times 10^{-4}, \quad A_{\text{CP}}^{\text{dir}}(B_s^0 \rightarrow J/\psi h_1(1415)) = 1.28_{-1.62}^{+1.91} \times 10^{-4}. \quad (51)$$

All the errors arising from various parameters in the above-mentioned have been added in quadrature. The dependence of $A_{\text{CP}}^{\text{dir}}(B^0 \rightarrow J/\psi h_1)$ on the mixing angle θ is shown in Fig. 6. It can be found that the direct CP asymmetries are too small to be observed, although they are relatively sensitive to θ at some specific range.

All of the aforementioned theoretical predictions in the PQCD approach are expected to be tested by LHCb, Belle-II and proposed CEPC experiments in the future. The relevant predictions for these experimental observables would be helpful to explore the dynamics involved in the $B^0 \rightarrow J/\psi h_1$ decays and to identify the inner structure or the components of the h_1 states.

IV. CONCLUSIONS AND SUMMARY

In this paper, we have calculated the $B^0 \rightarrow J/\psi h_1$ decays for the first time by using PQCD approach, where $h_1 = h_1(1170)$ and $h_1(1415)$ are treated as the mixtures of \tilde{h}_1 and \tilde{h}_8 with mixing angle θ in the singlet-octet basis. The observables of these decays are predicted. The NLO order corrections are considered in the calculation because the vertex corrections with the NLO Wilson coefficients contribute significantly to the color-suppressed decay modes. We take $\theta = 29.5^\circ$ as default input, and the effects of θ on the observables are discussed in detail. Our conclusions can be summarized briefly as following,

- The $B^0 \rightarrow J/\psi h_1$ decays have relatively large branching fractions, which are generally at the order of $\mathcal{O}(10^{-6} \sim 10^{-3})$, and thus are possible to be measured by the LHCb and Belle-II experiments in the near future. The measurements with high precision can provide useful information for basic nature of $h_1(1170)$ and $h_1(1415)$.

- Further considering the secondary decays, $(h_1(1415), f_1(1420)) \rightarrow K_S^0 K^+ \pi^-$, and comparing them with the LHCb data for $\mathcal{B}(B_s^0 \rightarrow J/\psi K_S^0 K^+ \pi^-)$, we find that the $h_1(1415)$ resonance serves possibly as a contributing state in the $m(K_S^0 K^\pm \pi^\mp)$ distribution.
- The branching fractions of $B^0 \rightarrow J/\psi h_1$ decays are very sensitive to the mixing angle, and thus can be used to test the values of θ . Several interesting ratios between the branching fractions of $B^0 \rightarrow J/\psi h_1$ decays, such as R_d^{SO} , R_s^{SO} , R_{ds}^{SO} , can effectively avoid large theoretical errors caused by the hadronic inputs, and thus would provide much stronger constraints on θ .
- All of the $B^0 \rightarrow J/\psi h_1$ decays are generally dominated by the longitudinal polarization contributions, namely, $f_L(B^0 \rightarrow J/\psi h_1) > 80\%$, with default input $\theta = 29.5^\circ$. The longitudinal fractions can be significantly reduced when some specific values, $\theta \sim 35^\circ, -55^\circ$, are taken. Therefore, the polarization fractions of $B^0 \rightarrow J/\psi h_1$ decays can provide restrict constraint on θ .
- Maybe the direct CP asymmetries of $B^0 \rightarrow J/\psi h_1$ decays are too small to be observed soon even if the effect of θ is considered.

ACKNOWLEDGMENTS

The work is supported by the National Natural Science Foundation of China (Grant Nos. 12275067, 11875033), Science and Technology R&D Program Joint Fund Project of Henan Province (Grant No.225200810030), Excellent Youth Foundation of Henan Province (Grant no. 212300410010), and National Key R&D Program of China (Grant No. 2023YFA1606000).

Appendix A: Specific derivation of angle calculations

Under the basis \tilde{h}_1 and \tilde{h}_8 , we can write the mass matrix as follows [4, 11],

$$\begin{pmatrix} \langle \tilde{h}_1 | H^2 | \tilde{h}_1 \rangle & \langle \tilde{h}_1 | H^2 | \tilde{h}_8 \rangle \\ \langle \tilde{h}_8 | H^2 | \tilde{h}_1 \rangle & \langle \tilde{h}_8 | H^2 | \tilde{h}_8 \rangle \end{pmatrix} = \begin{pmatrix} m_{\tilde{h}_1}^2 & m_{\tilde{h}_{18}}^2 \\ m_{\tilde{h}_{18}}^2 & m_{\tilde{h}_8}^2 \end{pmatrix}. \quad (\text{A1})$$

The mixing angle θ can be derived by diagonalizing the mass matrix, and the mass matrix diagonalized according to the following relation,

$$R(\theta) M^2 R(\theta)^{-1} = M_{diag}^2. \quad (\text{A2})$$

Therefore, one can obtain the physical masses of $h_1(1170)$ and $h_1(1415)$ states,

$$\begin{pmatrix} m_{h_1(1170)}^2 & 0 \\ 0 & m_{h_1(1415)}^2 \end{pmatrix} = \begin{pmatrix} \cos \theta & \sin \theta \\ -\sin \theta & \cos \theta \end{pmatrix} \begin{pmatrix} m_{\tilde{h}_1}^2 & m_{\tilde{h}_{18}}^2 \\ m_{\tilde{h}_{18}}^2 & m_{\tilde{h}_8}^2 \end{pmatrix} \begin{pmatrix} \cos \theta & -\sin \theta \\ \sin \theta & \cos \theta \end{pmatrix}. \quad (\text{A3})$$

Then, we have

$$m_{h_1(1170)}^2 \cos^2 \theta = m_{\tilde{h}_1}^2 \cos^2 \theta + m_{\tilde{h}_{18}}^2 \sin \theta \cos \theta, \quad (\text{A4})$$

$$m_{h_1(1415)}^2 \sin^2 \theta = m_{\tilde{h}_1}^2 \sin^2 \theta - m_{\tilde{h}_{18}}^2 \cos \theta \sin \theta, \quad (\text{A5})$$

$$m_{h_1(1170)}^2 \sin^2 \theta = m_{\tilde{h}_{18}}^2 \cos \theta \sin \theta + m_{\tilde{h}_8}^2 \sin^2 \theta, \quad (\text{A6})$$

$$m_{h_1(1415)}^2 \cos^2 \theta = -m_{\tilde{h}_{18}}^2 \sin \theta \cos \theta + m_{\tilde{h}_8}^2 \cos^2 \theta. \quad (\text{A7})$$

By utilizing Eqs. (A4)-(A7), the following relationship can be derived,

$$m_{\tilde{h}_1}^2 = m_{h_1(1415)}^2 \sin^2 \theta + m_{h_1(1170)}^2 \cos^2 \theta, \quad (\text{A8})$$

$$m_{\tilde{h}_8}^2 = m_{h_1(1415)}^2 \cos^2 \theta + m_{h_1(1170)}^2 \sin^2 \theta, \quad (\text{A9})$$

$$m_{\tilde{h}_{18}}^2 = -\frac{1}{2}(m_{h_1(1415)}^2 - m_{h_1(1170)}^2) \sin 2\theta. \quad (\text{A10})$$

After further collation and simplification, the following results can be obtained,

$$\cos^2 \theta = \frac{m_{\tilde{h}_8}^2 - m_{h_1(1170)}^2}{m_{h_1(1415)}^2 - m_{h_1(1170)}^2} = \frac{4m_{K_{1B}}^2 - m_{b_1}^2 - 3m_{h_1(1170)}^2}{3(m_{h_1(1415)}^2 - m_{h_1(1170)}^2)}, \quad (\text{A11})$$

$$\tan \theta = \frac{4m_{K_{1B}}^2 - m_{b_1}^2 - 3m_{h_1(1415)}^2}{2\sqrt{2}(m_{b_1}^2 - K_{1B}^2)}, \quad (\text{A12})$$

where, the Gell-Mann–Okubo mass relation, $m_{b_1}^2 + 3m_{h_8}^2 = 4m_{K_{1B}}^2$.

Appendix B: Meson wave functions and distribution amplitudes

Notice that, the process of B -meson decays into J/ψ plus light hadrons have been studied in the PQCD approach at the NLO accuracy [25, 30, 38]. Hence, in this article, the same wave functions and the related distribution amplitudes for the heavy B^0 and J/ψ mesons will not be presented one by one here and could be found in Ref. [30].

For the light axial-vector meson h_1 , the wave functions associated with the light-cone distribution amplitudes at both longitudinal and transverse polarizations have been given in the QCD

sum rule up to twist-3. Therefore, the wave function could be written as [24, 61],

$$\Phi_A^L(x) = \frac{1}{\sqrt{2N_c}} \gamma_5 \left\{ m_A \not{\epsilon}_L \phi_A(x) + \not{\epsilon}_L \not{P} \phi_A^t(x) + m_A \phi_A^s(x) \right\}_{\alpha\beta}, \quad (\text{B1})$$

$$\Phi_A^T(x) = \frac{1}{\sqrt{2N_c}} \gamma_5 \left\{ m_A \not{\epsilon}_T \phi_A^v(x) + \not{\epsilon}_T \not{P} \phi_A^T(x) + m_A i \epsilon_{\mu\nu\rho\sigma} \gamma_5 \gamma^\mu \not{\epsilon}_T^\nu n^\rho v^\sigma \phi_A^a(x) \right\}_{\alpha\beta}, \quad (\text{B2})$$

where ϵ_L and ϵ_T are the longitudinal and transverse polarization vectors of h_1 meson, x denotes the momentum fraction carried by quark in h_1 , $n = (1, 0, \mathbf{0}_T)$ and $v = (0, 1, \mathbf{0}_T)$ are dimensionless lightlike vectors, the Levi-Civita tensor $\epsilon^{\mu\nu\alpha\beta}$ is conventionally taken as $\epsilon^{0123} = 1$. With the twist-2 light-cone distribution amplitudes, i.e., $\phi_A(x)$ and $\phi_A^T(x)$, can be expanded as the Gegenbauer polynomials [61],

$$\phi_A(x) = \frac{3f_A}{\sqrt{2N_c}} x(1-x) \left[3a_1^\parallel (2x-1) \right], \quad (\text{B3})$$

$$\phi_A^T(x) = \frac{3f_A}{\sqrt{2N_c}} x(1-x) \left[1 + a_2^\perp \frac{3}{2} (5(2x-1)^2 - 1) \right]. \quad (\text{B4})$$

And the twist-3 light-cone distribution amplitudes will be used in the following form [61],

$$\phi_A^s(x) = \frac{3f_A}{2\sqrt{2N_c}} \frac{d}{dx} \left[x(1-x) \right], \quad \phi_A^t(x) = \frac{3f_A}{2\sqrt{2N_c}} \left[(2x-1)^2 \right], \quad (\text{B5})$$

$$\phi_A^v(x) = \frac{3f_A}{4\sqrt{2N_c}} \left[a_1^\parallel (2x-1)^3 \right], \quad \phi_A^a(x) = \frac{3f_A}{4\sqrt{2N_c}} \frac{d}{dx} \left[x(1-x) \left(a_1^\parallel (2x-1) \right) \right], \quad (\text{B6})$$

where f_A is the decay constant of the single-octet states $f_{\tilde{h}_{1,8}}$ and the Gegenbauer moments a_1^\parallel and a_2^\perp in Eqs. (B3)-(B6) at the renormalization scale $\mu=1$ GeV are as follows [24],

$$a_1^\parallel = \begin{cases} -1.95_{-0.35}^{+0.35} & \left(\text{for } \tilde{h}_8 \right), \\ -2.00_{-0.35}^{+0.35} & \left(\text{for } \tilde{h}_1 \right), \end{cases} \quad a_2^\perp = \begin{cases} 0.14_{-0.22}^{+0.22} & \left(\text{for } \tilde{h}_8 \right), \\ 0.18_{-0.22}^{+0.22} & \left(\text{for } \tilde{h}_1 \right). \end{cases} \quad (\text{B7})$$

-
- [1] K. Abe *et al.* [Belle], Phys. Rev. Lett. **87**, 091802 (2001).
- [2] K. Abe *et al.* [Belle], Phys. Rev. Lett. **87**, 161601 (2001).
- [3] L. Burakovsky and J. T. Goldman, Phys. Rev. D **56**, R1368-R1372 (1997).
- [4] H. Y. Cheng, Phys. Lett. B **707**, 116-120 (2012).
- [5] K. Chen, C. Q. Pang, X. Liu and T. Matsuki, Phys. Rev. D **91**, 074025 (2015).
- [6] R. L. Workman *et al.* [Particle Data Group], PTEP **2022**, 083C01 (2022).
- [7] Y. S. Amhis *et al.* [HFLAV], Phys. Rev. D **107**, 052008 (2023).
- [8] W. H. Liang, S. Sakai and E. Oset, Phys. Rev. D **99**, 094020 (2019).
- [9] X. Liu and Z. J. Xiao, J. Phys. G **38**, 035009 (2011).
- [10] X. Liu and Z. J. Xiao, Phys. Rev. D **81**, 074017 (2010).
- [11] M. C. Du and Q. Zhao, Phys. Rev. D **104**, 036008 (2021).
- [12] M. C. Du, Y. Cheng and Q. Zhao, Phys. Rev. D **106**, 054019 (2022).
- [13] M. Ablikim *et al.* [BESIII], Phys. Rev. D **91**, 112008 (2015).
- [14] M. Ablikim *et al.* [BESIII], Phys. Rev. D **98**, 072005 (2018).
- [15] M. Ablikim *et al.* [BESIII], Phys. Rev. D **105**, 072002 (2022).
- [16] S. Navas *et al.* [Particle Data Group], Phys. Rev. D **110**, 030001 (2024).
- [17] H. Y. Cheng, PoS **Hadron2013**, 090 (2013).
- [18] M. Suzuki, Phys. Rev. D **47**, 1252-1255 (1993).
- [19] H. G. Blundell, S. Godfrey and B. Phelps, Phys. Rev. D **53**, 3712-3722 (1996).
- [20] L. Burakovsky and J. T. Goldman, Phys. Rev. D **57**, 2879-2888 (1998).
- [21] H. Dag, A. Ozpineci, A. Cagil and G. Erkol, J. Phys. Conf. Ser. **348**, 012012 (2012).
- [22] F. Divotgey, L. Olbrich and F. Giacosa, Eur. Phys. J. A **49**, 135 (2013).
- [23] Y. Gao, Y. Zhang, B. Zheng, Z. H. Zhang, W. Yan and X. Li, [arXiv:1911.06967 [hep-ph]].
- [24] K. C. Yang, Nucl. Phys. B **776**, 187-257 (2007).
- [25] C. H. Chen and H. N. Li, Phys. Rev. D **71**, 114008 (2005).
- [26] J. W. Li and D. S. Du, Phys. Rev. D **78**, 074030 (2008).
- [27] J. W. Li, D. S. Du and C. D. Lu, Eur. Phys. J. C **72**, 2229 (2012).
- [28] X. Liu and Z. J. Xiao, Phys. Rev. D **89**, 097503 (2014).
- [29] X. Liu, Z. T. Zou, Y. Li and Z. J. Xiao, Phys. Rev. D **100**, 013006 (2019).
- [30] D. H. Yao, X. Liu, Z. T. Zou, Y. Li and Z. J. Xiao, Eur. Phys. J. C **83**, 13 (2023).
- [31] H. Y. Cheng and K. C. Yang, Phys. Rev. D **63**, 074011 (2001).
- [32] J. Sun, Z. Xiong, Y. Yang and G. Lu, Eur. Phys. J. C **73**, 2437 (2013).
- [33] Z. z. Song, C. Meng and K. T. Chao, Eur. Phys. J. C **36**, 365-370 (2004).
- [34] C. Meng, Y. J. Gao and K. T. Chao, Phys. Rev. D **87**, 074035 (2013).
- [35] H. n. Li and S. Mishima, JHEP **03**, 009 (2007).

- [36] M. Beneke and L. Vernazza, Nucl. Phys. B **811**, 155-181 (2009).
- [37] P. Colangelo, F. De Fazio and W. Wang, Phys. Rev. D **83**, 094027 (2011).
- [38] X. Liu, W. Wang and Y. Xie, Phys. Rev. D **89**, 094010 (2014).
- [39] W. F. Wang, H. n. Li, W. Wang and C. D. Lü, Phys. Rev. D **91**, 094024 (2015).
- [40] Z. Q. Zhang, H. Guo and S. Y. Wang, Eur. Phys. J. C **78**, 219 (2018).
- [41] Z. Rui, Y. Li and H. Li, Eur. Phys. J. C **79**, 792 (2019).
- [42] Y. Q. Li, M. K. Jia and Z. Rui, Chin. Phys. C **44**, 113104 (2020).
- [43] X. Liu, H. n. Li and Z. J. Xiao, Phys. Rev. D **97**, 113001 (2018).
- [44] X. Liu, H. n. Li and Z. J. Xiao, Phys. Lett. B **811**, 135892 (2020).
- [45] X. Liu, Phys. Rev. D **108**, 096006 (2023).
- [46] Y. Y. Keum, H. n. Li and A. I. Sanda, Phys. Lett. B **504**, 6-14 (2001).
- [47] Y. Y. Keum, H. N. Li and A. I. Sanda, Phys. Rev. D **63**, 054008 (2001).
- [48] C. D. Lu, K. Ukai and M. Z. Yang, Phys. Rev. D **63**, 074009 (2001).
- [49] C. D. Lu and M. Z. Yang, Eur. Phys. J. C **23**, 275-287 (2002).
- [50] A. Ali, G. Kramer, Y. Li, C. D. Lu, Y. L. Shen, W. Wang and Y. M. Wang, Phys. Rev. D **76**, 074018 (2007).
- [51] J. Chai, S. Cheng, Y. h. Ju, D. C. Yan, C. D. Lü and Z. J. Xiao, Chin. Phys. C **46**, 123103 (2022).
- [52] Z. J. Xiao, D. C. Yan and X. Liu, Nucl. Phys. B **953**, 114954 (2020).
- [53] J. L. Ren, M. Q. Li, X. Liu, Z. T. Zou, Y. Li and Z. J. Xiao, Eur. Phys. J. C **84**, 358 (2024).
- [54] G. Buchalla, A. J. Buras and M. E. Lautenbacher, Rev. Mod. Phys. **68**, 1125-1144 (1996).
- [55] Z. J. Xiao, Z. Q. Zhang, X. Liu and L. B. Guo, Phys. Rev. D **78**, 114001 (2008).
- [56] L. Wolfenstein, Phys. Rev. Lett. **51**, 1945 (1983).
- [57] R. C. Verma, J. Phys. G **39**, 025005 (2012).
- [58] R. Aaij *et al.* [LHCb], JHEP **07**, 140 (2014).
- [59] R. Fleischer, R. Knegjens and G. Ricciardi, Eur. Phys. J. C **71**, 1832 (2011).
- [60] M. Beneke, J. Rohrer and D. Yang, Nucl. Phys. B **774**, 64-101 (2007).
- [61] R. H. Li, C. D. Lu and W. Wang, Phys. Rev. D **79**, 034014 (2009).